RESEARCH ARTICLE

The BTK Inhibitor ARQ 531 Targets Ibrutinib-Resistant CLL and Richter Transformation

Sean D. Reiff[1,2], Rose Mantel[1], Lisa L. Smith[1], J.T. Greene[1], Elizabeth M. Muhowski[3], Catherine A. Fabian[1], Virginia M. Goettl[1], Minh Tran[1], Bonnie K. Harrington[1], Kerry A. Rogers[1], Farrukh T. Awan[1], Kami Maddocks[1], Leslie Andritsos[1], Amy M. Lehman[4], Deepa Sampath[1], Rosa Lapalombella[1], Sudharshan Eathiraj[5], Giovanni Abbadessa[5], Brian Schwartz[5], Amy J. Johnson[1,3], John C. Byrd[1,3], and Jennifer A. Woyach[1,3]

ABSTRACT

Targeted inhibition of Bruton tyrosine kinase (BTK) with the irreversible inhibitor ibrutinib has improved outcomes for patients with hematologic malignancies, including chronic lymphocytic leukemia (CLL). Here, we describe preclinical investigations of ARQ 531, a potent, reversible inhibitor of BTK with additional activity against Src family kinases and kinases related to ERK signaling. We hypothesized that targeting additional kinases would improve global inhibition of signaling pathways, producing more robust responses. *In vitro* treatment of patient CLL cells with ARQ 531 decreases BTK-mediated functions including B-cell receptor (BCR) signaling, viability, migration, CD40 and CD86 expression, and NF-κB gene transcription. *In vivo*, ARQ 531 was found to increase survival over ibrutinib in a murine Eμ-TCL1 engraftment model of CLL and a murine Eμ-MYC/TCL1 engraftment model resembling Richter transformation. Additionally, ARQ 531 inhibits CLL cell survival and suppresses BCR-mediated activation of C481S BTK and PLCγ2 mutants, which facilitate clinical resistance to ibrutinib.

SIGNIFICANCE: This study characterizes a rationally designed kinase inhibitor with efficacy in models recapitulating the most common mechanisms of acquired resistance to ibrutinib. Reversible BTK inhibition is a promising strategy to combat progressive CLL, and multikinase inhibition demonstrates superior efficacy to targeted ibrutinib therapy in the setting of Richter transformation. *Cancer Discov; 8(10); 1300–15. ©2018 AACR.*

[1]Department of Internal Medicine, Division of Hematology, Comprehensive Cancer Center, The Ohio State University, Columbus, Ohio. [2]Medical Scientist Training Program, The Ohio State University, Columbus, Ohio. [3]Division of Pharmaceutics, College of Pharmacy, The Ohio State University, Columbus, Ohio. [4]Center for Biostatistics, The Ohio State University, Columbus, Ohio. [5]ArQule, One Wall Street, Burlington, Massachusetts.

Note: Supplementary data for this article are available at Cancer Discovery Online (http://cancerdiscovery.aacrjournals.org/).

Current address for Giovanni Abbadessa: Sanofi Genzyme; and current address for Amy J. Johnson: Janssen Research and Development.

Corresponding Author: Jennifer A. Woyach, The Ohio State University, 410 W. 12th Avenue, Columbus, OH 43210. Phone: 614-685-5667; Fax: 614-293-7484; E-mail: Jennifer.woyach@osumc.edu

doi: 10.1158/2159-8290.CD-17-1409

INTRODUCTION

Recent appreciation for the extent to which Bruton tyrosine kinase (BTK) drives select hematologic malignancies such as chronic lymphocytic leukemia (CLL; refs. 1, 2) has spurred the development of targeted BTK inhibitors, most notably the irreversible inhibitor ibrutinib (3–8). Several pathways that work to increase the survival and proliferation of CLL B cells converge proximally on BTK (9); these pathways are initiated at the B-cell receptor (BCR), Toll-like receptors (10, 11), and multiple chemokine receptors (12, 13), making BTK an attractive therapeutic target. BTK is overexpressed at the transcript and protein level in CLL B cells compared with healthy donors, leading to constitutive BCR activation (14). *In vitro*, BTK inhibition induces CLL cytotoxicity, decreases NF-κB–dependent transcription, and abrogates chemokine-mediated migration of CLL cells to protective lymphoid microenvironments (14, 15). Clinically, ibrutinib produces durable responses with manageable drug-related toxicities in the majority of patients with CLL (16, 17). In the longest follow-up of patients treated with ibrutinib, the 5-year progression-free survival (PFS) rate was estimated to be 92% for treatment-naïve patients, whereas the median PFS for patients with relapsed/refractory disease was 52 months (16). Ibrutinib has broad regulatory approval for marketing in patients with CLL and is clinically effective regardless of most traditional prognostic factors, although complex karyotype, del(17p13.1), and age younger than 65 years are risk factors for late relapse (17).

Despite its initial clinical benefit for most patients, resistance to ibrutinib continues to emerge as more patients are being treated and follow-up time extends. Relapse on ibrutinib arises via Richter transformation to aggressive lymphoma, which occurs early in treatment, and CLL progression, which typically occurs beyond 1 to 2 years of therapy (17–19). Unfortunately, patients who relapse on ibrutinib have poor survival and limited therapeutic options (17, 19, 20–22), particularly those with Richter transformation. Among patients who develop progressive CLL on ibrutinib, approximately 86% acquire mutations in *BTK* and/or *PLCγ2*, BTK's immediate downstream partner (17, 19). *BTK* mutations associated with ibrutinib resistance occur at the C481 amino acid to which

ibrutinib irreversibly binds (23, 24), whereas *PLCγ2* mutations occur preferentially in the autoinhibitory domain of PLCγ2 (25, 26). The observation that resistance to ibrutinib is most frequently facilitated by mutation of BTK or its downstream partner implies that BTK function is necessary for the perpetuation of CLL and suggests that this pathway remains a relevant target in patients who relapse on ibrutinib. Therefore, an ongoing need exists to develop BTK targeting therapies for the population of patients with CLL whose disease progresses on ibrutinib therapy due to Richter transformation or ibrutinib-resistant CLL.

Patients with CLL who experience Richter transformation while on ibrutinib have dismal survival of less than 6 months (17, 20–22). This type of resistance is generally not associated with *BTK* or *PLCγ2* mutations (18). Recently, our laboratory developed a transgenic mouse model, which spontaneously develops an aggressive B-cell lymphoma resembling Richter transformation on the background of CLL (27). These mice overexpress MYC via an Eμ enhancer sequence in addition to overexpression of TCL1. The transgenic Eμ-TCL1 is a standard CLL mouse model that specifically overexpresses the *TCL1* oncogene via a B cell–specific IgVH promoter and Eμ enhancer (28). The spontaneous CLL-like leukemia that develops is dependent on BCR signaling and BTK (2, 28). The Eμ-MYC/TCL1 mouse utilized in this study fills an unmet need for murine models that recapitulate the disease phenotype of Richter transformation.

Although selective inhibition of BTK is effective in CLL, the extent to which concurrent inhibition of additional kinases may enhance treatment response is unknown. Here, we characterize ARQ 531, a potent, ATP-competitive, reversible inhibitor of BTK and several additional kinases important to the viability, proliferation, activation, and motility of CLL B cells. Among these targets are LYN, the kinase that initiates intracellular BCR signaling, and MEK1, which directly activates ERK leading to B-cell proliferation. Additionally, the activity of ARQ 531 is not predicated upon its ability to irreversibly bind the C481 amino acid of BTK, which is commonly mutated in patients who develop resistance to ibrutinib. Therefore, we hypothesized that ARQ 531 would be effective in both BTK inhibitor–naïve CLL and ibrutinib-resistant CLL arising from the C481S BTK and/or activating *PLCγ2* mutations. Herein, we demonstrate the preclinical efficacy of this molecule.

RESULTS

ARQ 531 Is a Potent Inhibitor of BCR Signaling

ARQ 531 was designed as a reversible, orally bioavailable, ATP-competitive inhibitor of BTK (Fig. 1A). Crystal structure of BTK in complex with ARQ 531 at 1.1 Å resolution shows that ARQ 531 inhibits BTK by competing with ATP (Fig. 1B). The core pyrrolopyrimidine moiety forms bidentate hydrogen bonding with the hinge backbone of E475 and Y476 residues, and the chlorine atom is positioned between the A428 and K430 side chains. Similar to ibrutinib (29), the phenoxyphenyl group occupies the hydrophobic pocket of the ATP binding region. The polar tetrahydropyran methanol side chain is exposed to the solvent area and facilitates water-mediated extensive hydrogen bonding network. Importantly, ARQ 531 does not interact with C481, suggesting that C481S mutation would not affect binding.

Initial determination of the kinase inhibitory profile of ARQ 531 was performed via a biochemical kinase screen (Supplementary Table S1). ARQ 531 possesses nanomolar potency against TEC family kinases including the target kinase BTK as well as several Src family kinases and MEK1 (Fig. 1C and D). Following a single oral gavage administration of ARQ 531 at 10 mg/kg in cynomolgus monkeys (*Macaca fascicularis*), ARQ 531 was absorbed with a mean T_{max} of 6.67 hours (minimum 4.00 hours and maximum 12.0 hours; Supplementary Fig. S1). The mean C_{max} and AUC_{0-t} values were 4,400 ng/mL and 82,700 ng·h/mL, respectively. AUC_{0-inf} and $t_{1/2}$ were not calculated due to the lack of a clear elimination phase. At 24 hours, about 75% of its peak concentration can be measured in the plasma, suggesting that ARQ 531 exhibits long half-life pharmacokinetic (PK) properties.

To confirm inhibition of BCR-associated kinases in a cellular model, primary CLL cells were treated with escalating doses of ARQ 531. As expected, BCR-mediated activation of BTK, AKT, and ERK was inhibited in a dose-dependent manner by ARQ 531 (Fig. 2A and B). Although ARQ 531 and ibrutinib comparably decreased BTK and AKT phosphorylation, ARQ 531 decreased ERK phosphorylation more effectively than ibrutinib, likely due to predicted inhibition of MEK1. We also found that phosphorylation of Src family kinases and SYK was also inhibited by ARQ 531, but not by ibrutinib, in patient-derived primary CLL cells (Fig. 2C). After observing this differential ability to inhibit kinases upstream of BTK in the BCR pathway, we sought to determine if the Y551 amino acid of BTK, which is transphosphorylated by SYK leading to autophosphorylation of Y223 and BTK kinase activity, is affected by ARQ 531. Indeed, we found that both the Y551 and Y223 activation sites of BTK were dephosphorylated by ARQ 531, whereas only the Y223 autoactivation site of BTK was dephosphorylated with ibrutinib treatment (Fig. 2D).

ARQ 531 Is Cytotoxic to CLL Cells *In Vitro*

We next sought to determine if ARQ 531 was cytotoxic to CLL cells. At 48 hours, the viability of CLL cells treated with continuous exposure to 0.1, 1.0, or 10.0 μmol/L ARQ 531 was found to decrease in a dose-dependent manner by 19% ($P = 0.001$), 40% ($P < 0.001$), and 59% ($P < 0.001$), respectively (Fig. 3A). Additionally, we evaluated direct cytotoxicity in primary CLL cells treated with ARQ 531 for 2 hours followed by drug washout and media replacement. Cytotoxicity following washout did not significantly differ from the continuous drug exposure experiment ($P = 0.859$), suggesting that ARQ 531 maintains sufficient residency of its targets to elicit cytotoxicity even with short drug exposure (Fig. 3B).

ARQ 531 Abrogates CpG-Mediated Activation and Chemokine-Induced Migration of CLL Cells

BTK activation has been shown to increase NF-κB activity and thus CLL cell activation (31), events that can be blocked by ibrutinib (14). To determine whether ARQ 531 similarly affects NF-κB target genes, we performed real-time PCR in primary CLL cells following treatment with ARQ 531 and ibrutinib. ARQ 531 significantly decreased transcription of *MYC*, *MCL1*, and *CD40* compared with vehicle by 73%

A

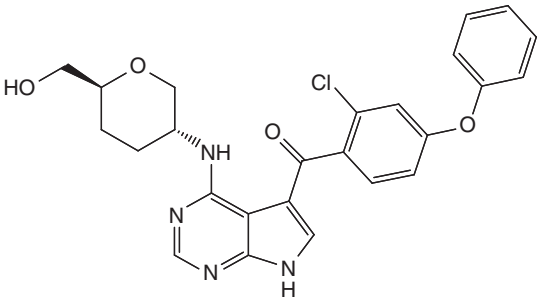

B

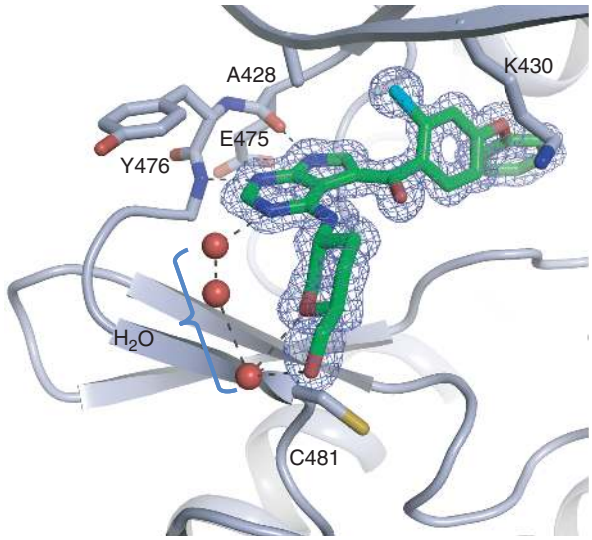

C

Kinase	Biochemical inhibition IC_{50} (nmol/L)
BRK	2.5
LCK*	3.9
YES*	4.2
BMX**	5.2
TEC**	5.8
BLK*	9.7
TRKB***	12
TRKA***	13
HCK*	18
LYNa*	19
TRKC***	19
FGR*	26
TIE2	29
FYN*	32
RAF1	35
TXK**	36
CSK	45
FRK*	48
MEK1	599
ITK	>10,000

*Src family kinases
**TEK family kinases
***TRK family kinases

D

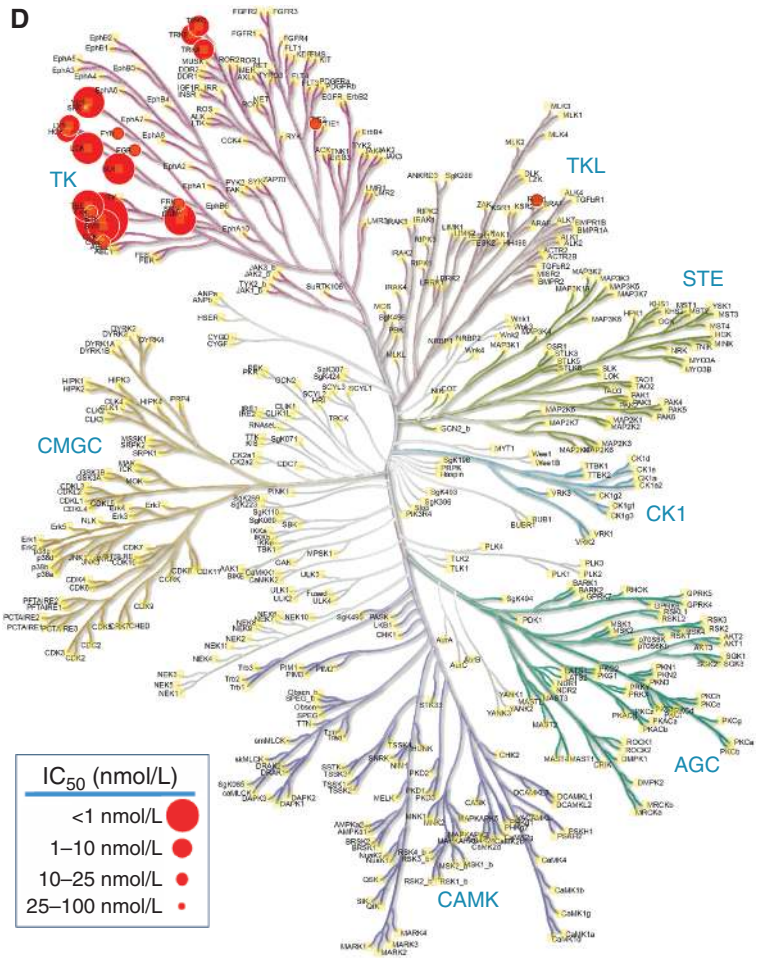

Figure 1. Structure and inhibitory profile of ARQ 531. **A,** Chemical structure of ARQ 531. **B,** 1.1 angstrom resolution crystal structure of ARQ 531 in complex with BTK. ARQ 531 occupies the ATP binding pocket and the solvent exposed side chain forms water-mediated hydrogen bond network (PDB ID: 6E4F). **C,** Kinases demonstrating greater than 50% inhibition at 200 nmol/L ARQ 531 were subjected to IC_{50} determination at a physiologic 1 mmol/L ATP concentration. **D,** IC_{50} values from **C** were plotted in a representation of the human kinome. Representation was generated using KinMap (30). Illustration reproduced courtesy of Cell Signaling Technology, Inc. (www.cellsignal.com).

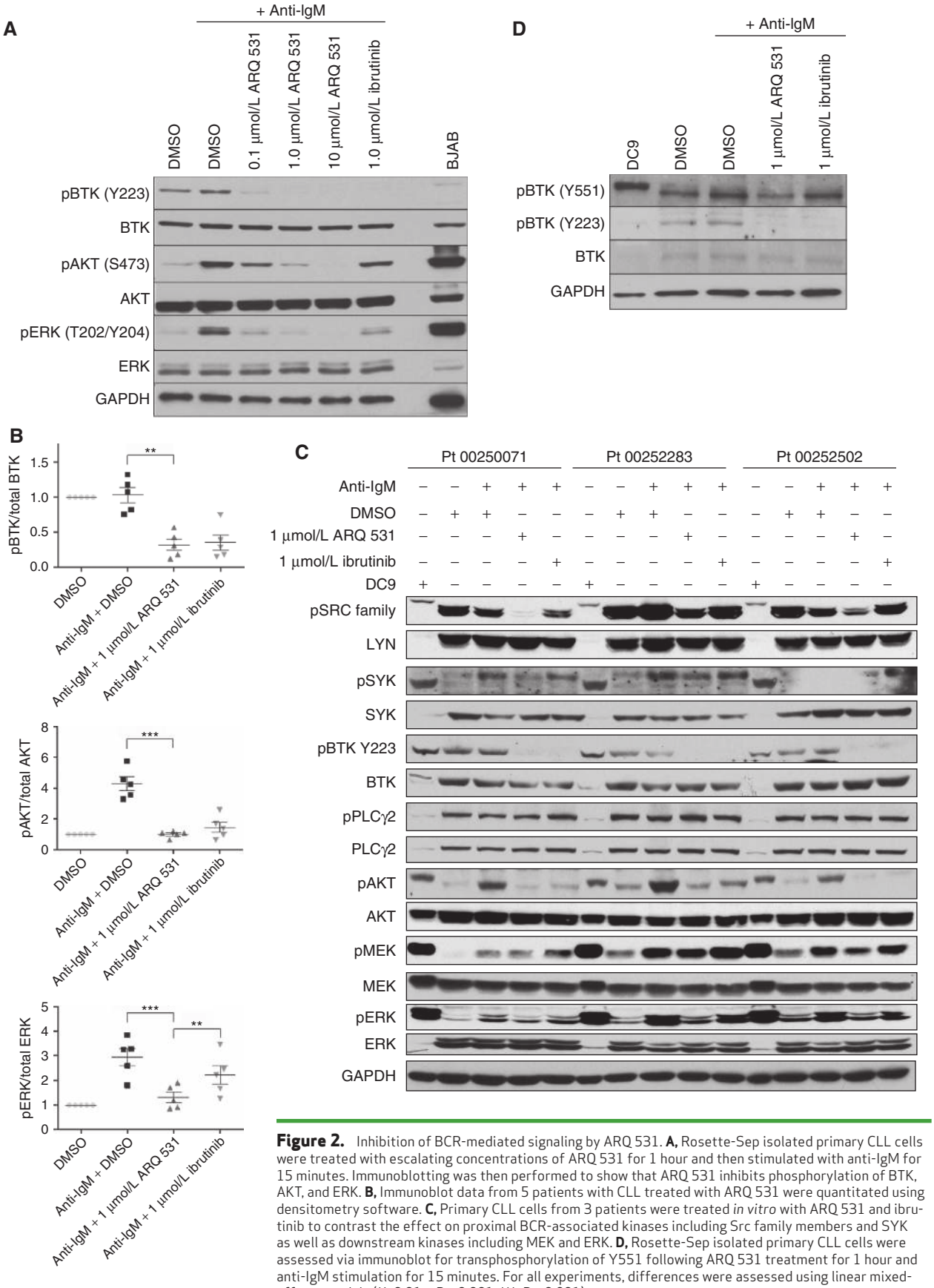

Figure 2. Inhibition of BCR-mediated signaling by ARQ 531. **A,** Rosette-Sep isolated primary CLL cells were treated with escalating concentrations of ARQ 531 for 1 hour and then stimulated with anti-IgM for 15 minutes. Immunoblotting was then performed to show that ARQ 531 inhibits phosphorylation of BTK, AKT, and ERK. **B,** Immunoblot data from 5 patients with CLL treated with ARQ 531 were quantitated using densitometry software. **C,** Primary CLL cells from 3 patients were treated *in vitro* with ARQ 531 and ibrutinib to contrast the effect on proximal BCR-associated kinases including Src family members and SYK as well as downstream kinases including MEK and ERK. **D,** Rosette-Sep isolated primary CLL cells were assessed via immunoblot for transphosphorylation of Y551 following ARQ 531 treatment for 1 hour and anti-IgM stimulation for 15 minutes. For all experiments, differences were assessed using linear mixed-effects models (**, $0.01 \geq P \geq 0.001$; ***, $P < 0.001$).

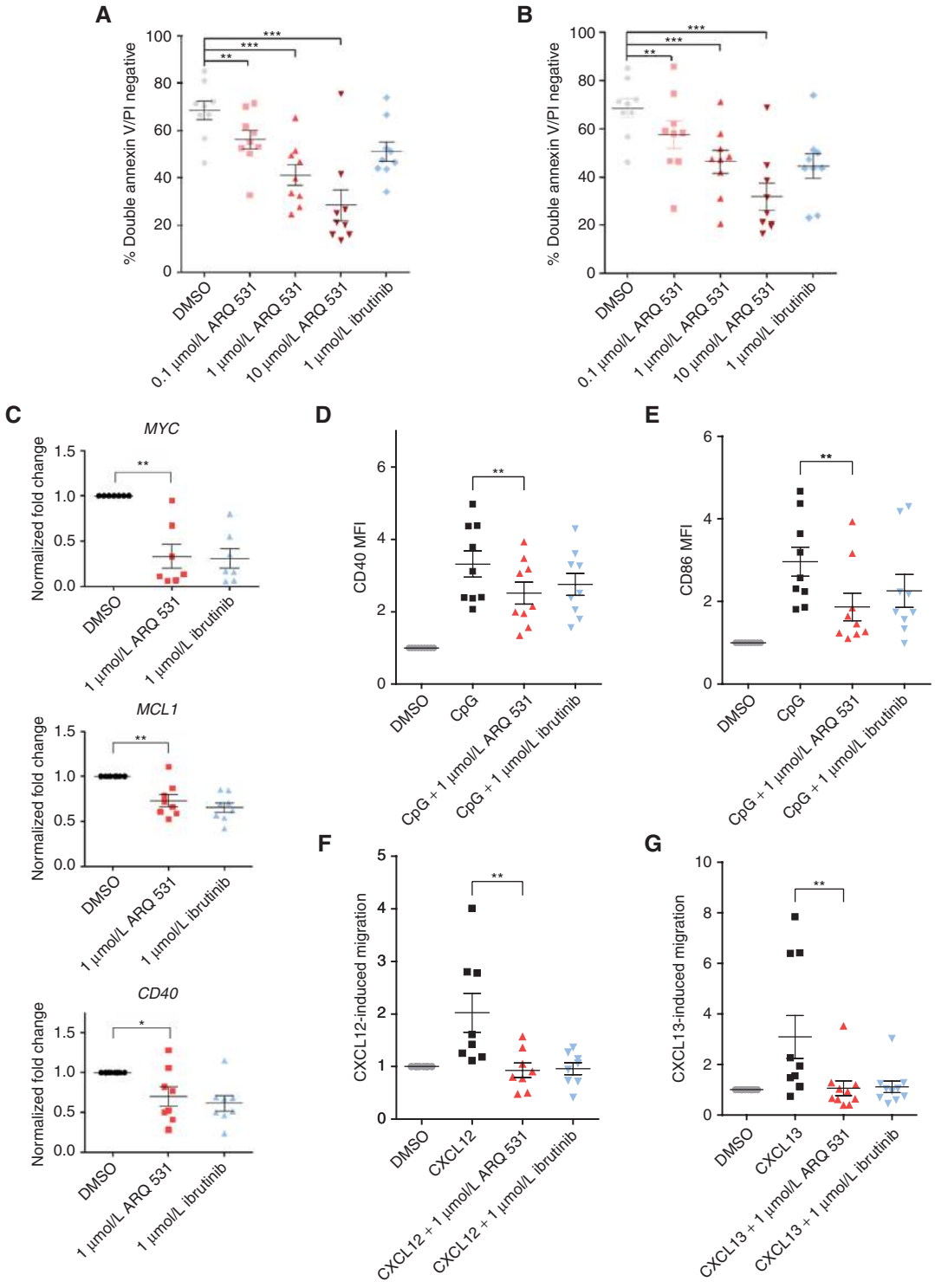

Figure 3. ARQ 531 is cytotoxic to CLL cells, decreases NF-κB function, and inhibits migration. **A,** Primary CLL cells were continuously treated with increasing concentrations of ARQ 531 for 48 hours to assess cytotoxicity via annexin V/propidium iodide (PI) staining and flow cytometry ($n = 9$). **B,** Primary CLL cells were treated daily with ARQ 531 for 2 hours followed by drug washout and media replacement in order to simulate clearance of the reversible BTK inhibitor ARQ 531 ($n = 9$). **C,** Transcriptional expression of *MYC*, *CD40*, and *MCL1* in CLL cells was assessed via real-time PCR following 72 hours of treatment with 1 μmol/L ARQ 531 ($n = 7$ for *MYC*; $n = 8$ for *MCL1* and *CD40*). **D** and **E,** The NF-κB–dependent activation markers CD40 and CD86 were measured via flow cytometry 48 hours following treatment with 1 μmol/L ARQ 531 and 3.2 μmol/L CpG in CLL B cells ($n = 9$). MFI, mean fluorescence intensity. **F** and **G,** The number of CLL cells migrating through an 8.0-μm transwell insert toward the chemokines CXCL12 and CXCL13 was counted by flow cytometry ($n = 8$ for CXCL12; $n = 9$ for CXCL13). Differences were assessed using linear mixed-effects models (*, $0.05 \geq P > 0.01$; **, $0.01 \geq P \geq 0.001$; ***, $P < 0.001$).

(P = 0.003), 23% (P = 0.003), and 40% (P = 0.027), respectively (Fig. 3C). As well, *in vitro* treatment of CLL cells with 1 μmol/L ARQ 531 for 48 hours decreased CpG-induced upregulation of CD40 and CD86 by 25% (P = 0.006) and 40% (P = 0.001), respectively (Fig. 3D and E). We next investigated if ARQ 531 inhibits migration of CLL cells toward cytokines (CXCL12 and CXCL13) secreted by the protective marrow microenvironment (32, 33). Using a transwell assay system, we found that ARQ 531 decreased migration of primary CLL cells toward CXCL12 by 51% (P = 0.002) and CXCL13 by 66% (P = 0.001; Fig. 3F and G).

ARQ 531 Is Superior to Ibrutinib in the Eμ-TCL1 Engraftment Mouse Model

We and others have demonstrated that the Eμ-TCL1 mouse model of CLL displays active BCR signaling and responds to treatment with the BTK inhibitors ibrutinib and acalabrutinib (13, 34, 35). Following the establishment of leukemia in an Eμ-TCL1 adaptive transfer model, we randomized mice to treatment with vehicle (n = 14), 25 mg/kg ibrutinib (n = 6), 50 mg/kg ARQ 531 (n = 14), or 75 mg/kg ARQ 531 (n = 14) given by daily oral gavage. PK and pharmacodynamic parameters are distinct for ARQ 531 and ibrutinib (36–38); therefore, it is challenging to predict dose equivalency to achieve comparable PK parameters in mice. Moreover, binding mechanisms of these drugs are also different, covalent irreversible ibrutinib versus noncovalent reversible ARQ 531; hence, identical doses would be unlikely to produce similar full and sustained *in vivo* pBTK inhibition. To overcome these limitations, ibrutinib and ARQ 531 were dosed at levels that would result in maximum pBTK inhibition and not be toxic to mice. A previous study showed a dose-dependent efficacy of ibrutinib in an Eμ-TCL1 adoptive transfer mouse model, 25 mg/kg of ibrutinib was found to be an optimal dose that does not cause any noticeable toxicity (32), and BTK was fully occupied by ibrutinib at this dose; hence, 25 mg/kg ibrutinib was selected for the current study. *In vivo* target engagement analysis of ARQ 531 in the mouse xenograft tumor model suggested that adequate pBTK inhibition in mouse can be achieved at 50 to 75 mg/kg dose ranges, and, therefore, these 2 doses were selected for efficacy studies.

ARQ 531 given at either 50 or 75 mg/kg was found to significantly improve survival over ibrutinib treatment (P = 0.044 and P = 0.009, respectively). Median survival of mice treated with vehicle, ibrutinib, and ARQ 531 was 36 days, 53 days, and not reached by 74 days, respectively, for both dose levels (Fig. 4A). ARQ 531 was discontinued on day 74 to assess the rate of disease progression. Following observation off ARQ 531 therapy, mice rapidly died of progressive disease, with a final median survival of 76 days for the 50 mg/kg ARQ 531 cohort and 78 days for the 75 mg/kg ARQ 531 cohort. Mice receiving ARQ 531 had lower blood lymphocyte counts on microscopic examination compared with those treated with vehicle or ibrutinib (Fig. 4B). In a cohort of mice sacrificed 2 weeks after the initiation of therapy, splenic weight was significantly reduced in mice treated with ARQ 531 compared with vehicle (P = 0.001 for 50 mg/kg and P < 0.001 for 75 mg/kg; Fig. 4C). Collectively, these studies establish the superior efficacy of ARQ 531 in the Eμ-TCL1 transgenic mouse model of CLL as compared with ibrutinib.

ARQ 531 Is Effective in a Murine Model of Richter Transformation

Given the poor survival for patients with CLL whose disease progresses to Richter transformation, we next investigated if ARQ 531 demonstrates efficacy in a murine model of aggressive lymphoma that we have recently described (27), in which ibrutinib is ineffective. B cells isolated from the spleen of an Eμ-MYC/TCL1 mouse were engrafted into C57BL/6 mice via tail-vein injection followed by treatment 10 days after engraftment. A dose of 75 mg/kg ARQ 531 prolonged survival in this model with a median survival of 47 days compared with ibrutinib (median survival, 38 days; P = 0.036) and vehicle treatment (median survival, 35.5 days; P = 0.008; Fig. 5A). Additionally, the percentage of $CD19^+$ cells in the peripheral blood of these mice was lower throughout the course of the study in the cohort treated with ARQ 531 compared with mice treated with either ibrutinib or vehicle (Fig. 5B).

ARQ 531 Maintains Efficacy in Cells with C481S-Mutated BTK

We hypothesized that because ARQ 531 does not require stabilization from the C481 amino acid within BTK's ATP binding domain that this molecule would possess inhibitory activity against C481S BTK mutations which mediate clinical ibrutinib resistance. To determine the activity of ARQ 531 against C481S BTK, we performed a biochemical kinase assay utilizing recombinant BTK protein and found that the IC_{50} of ARQ 531 was similar for wild-type and C481S BTK (0.85 nmol/L and 0.39 nmol/L, respectively). ARQ 531 displayed slow-on and slow-off binding kinetics by surface plasmon resonance with a binding constant of 5 nmol/L (Supplementary Table S2). The residence time calculated from the dissociation rate was 51 to 59 minutes. As expected, the covalent inhibitor ibrutinib showed robust binding affinity with significantly longer residence time with BTK. The cocrystal structure of ARQ 531 with BTK reveals that the sulfhydryl side chain of C481 residue does not participate in direct binding. However, this residue is critical for irreversible binding of ibrutinib. The binding constant and residence time of ARQ 531 with the mutant BTK was comparable to the wild-type BTK. Consistent with the previous report (23), the BTK C481S mutation severely abrogated the off-rate kinetics of ibrutinib, dramatically affecting the binding affinity and the residence time. BTK C481S mutation also alters the binding mechanism of ibrutinib to a reversible mode.

We next evaluated ARQ 531 in a $BTK^{-/-}$ HEK293T cell line transfected with wild-type or C481S BTK. ARQ 531 inhibited both wild-type and C481S-mutated BTK in this system, whereas ibrutinib demonstrated efficacy only against wild-type BTK (Fig. 6A; Supplementary Fig. S2). Next, we evaluated ARQ 531 *in vitro* in CLL cells isolated from a patient with C481S BTK acquired following ibrutinib therapy. We found that ARQ 531 inhibited activation of Src family members, BTK, AKT, and ERK similarly in baseline and relapse samples (Fig. 6B). Finally, we determined the cytotoxicity of ARQ 531 against ibrutinib-resistant primary CLL cells expressing C481S BTK. At 72 hours, ARQ 531 mediated significant cytotoxicity (28% decrease compared with vehicle, P = 0.002),

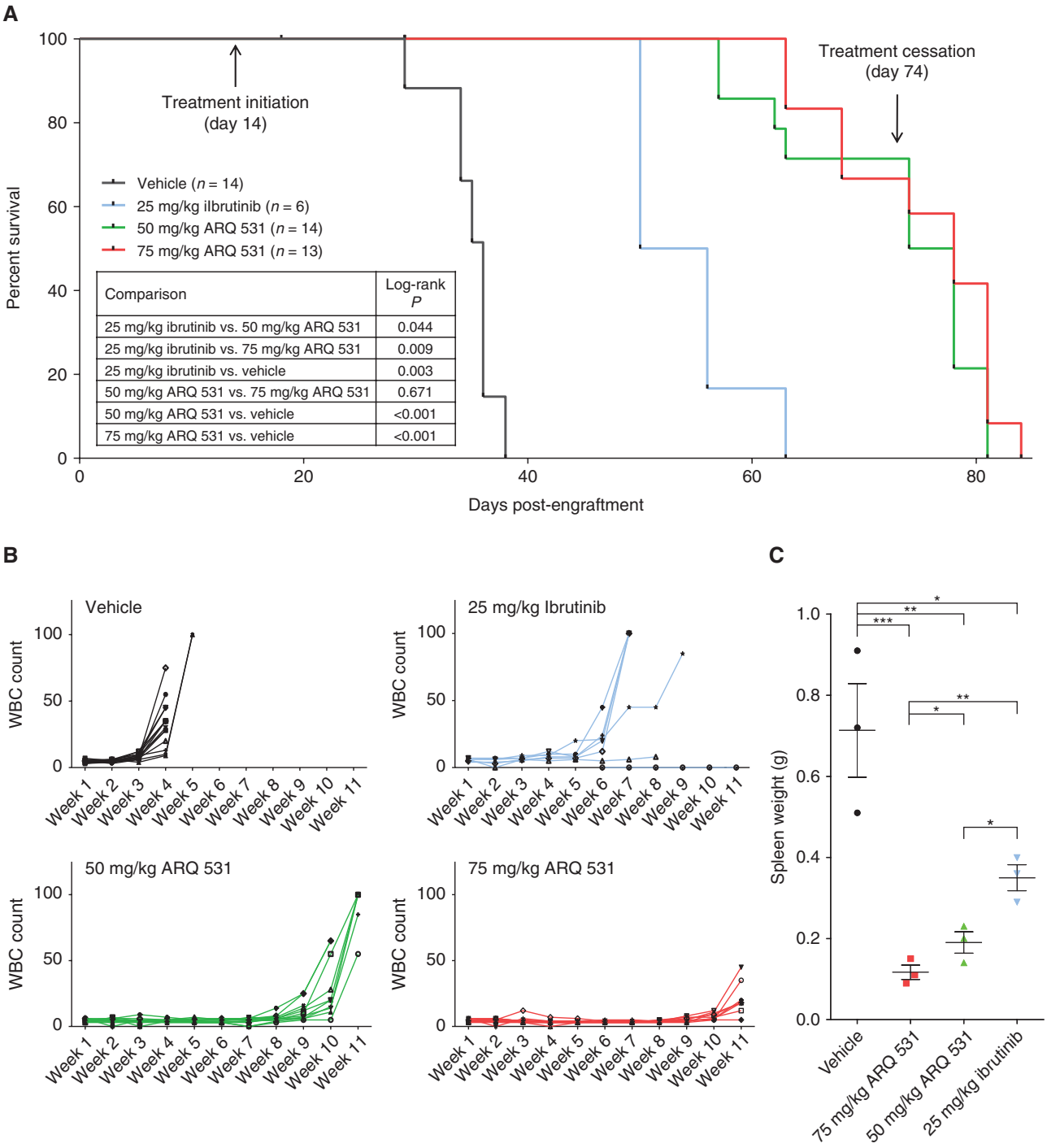

Comparison	Log-rank *P*
25 mg/kg ibrutinib vs. 50 mg/kg ARQ 531	0.044
25 mg/kg ibrutinib vs. 75 mg/kg ARQ 531	0.009
25 mg/kg ibrutinib vs. vehicle	0.003
50 mg/kg ARQ 531 vs. 75 mg/kg ARQ 531	0.671
50 mg/kg ARQ 531 vs. vehicle	<0.001
75 mg/kg ARQ 531 vs. vehicle	<0.001

Figure 4. ARQ 531 improves survival in the Eμ-TCL1 engraftment model compared with ibrutinib. **A,** C57BL/6 mice engrafted with Eμ-TCL1 leukocytes via tail-vein injection were treated with ARQ 531 for 60 days via daily oral gavage and monitored for survival and drug-induced toxicity. Survival curves were estimated using the Kaplan–Meier method and curve differences among groups were assessed using the log-rank test. **B,** White blood cell (WBC) counts were measured weekly by microscopic examination. **C,** A cohort of mice were sacrificed after 2 weeks of treatment, and spleens were weighed to measure disease progression ($n = 3$ in each group). ANOVA was used to compare spleen weight among groups (*, $0.05 \geq P > 0.01$; **, $0.01 \geq P \geq 0.001$; ***, $P < 0.001$).

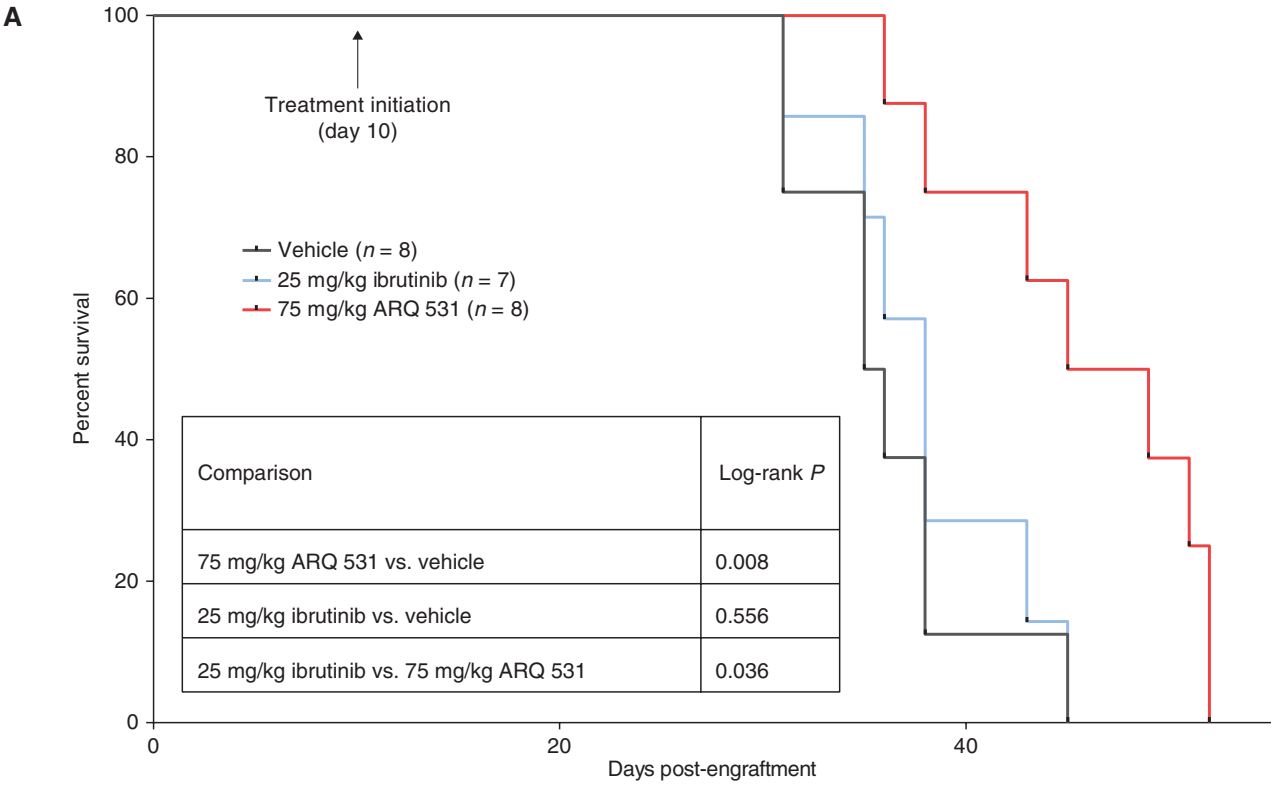

Comparison	Log-rank *P*
75 mg/kg ARQ 531 vs. vehicle	0.008
25 mg/kg ibrutinib vs. vehicle	0.556
25 mg/kg ibrutinib vs. 75 mg/kg ARQ 531	0.036

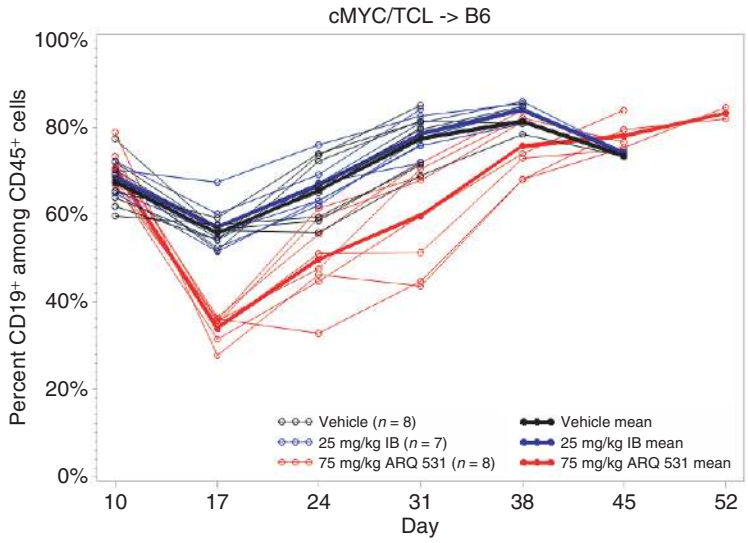

Day	Comparison	Estimated difference	95% CI	*P*
10	ARQ 531 vs. ibrutinib	2.53	(–3.35, 8.41)	>0.999
	ARQ 531 vs. vehicle	3.2	(–2.47, 8.87)	>0.999
	Ibrutinib vs. vehicle	0.67	(–5.21, 6.55)	>0.999
17	ARQ 531 vs. ibrutinib	–22.85	(–28.73, –16.97)	<0.001
	ARQ 531 vs. vehicle	–21.72	(–27.39, –16.05)	<0.001
	Ibrutinib vs. vehicle	1.13	(–4.75, 7.01)	>0.999
24	ARQ 531 vs. ibrutinib	–16.91	(–22.79, –11.03)	<0.001
	ARQ 531 vs. vehicle	–15.89	(–21.55, –10.22)	<0.001
	Ibrutinib vs. vehicle	1.03	(–4.85, 6.91)	>0.999
31	ARQ 531 vs. ibrutinib	–18.49	(–24.37, –12.61)	<0.001
	ARQ 531 vs. vehicle	–17.72	(–23.38, –12.05)	<0.001
	Ibrutinib vs. vehicle	0.78	(–5.1, 6.66)	>0.999

Figure 5. ARQ 531 improves survival in the Eμ-MYC/TCL1 model compared with ibrutinib. **A,** C57BL/6 mice engrafted via tail-vein injection with Eμ-MYC/TCL1 leukocytes were treated with ARQ 531 via daily oral gavage starting 10 days after engraftment and monitored for survival. **B,** Percent CD19+ leukocytes collected from weekly bleeding were measured via flow cytometry. Survival curves were estimated using the Kaplan–Meier method and curve differences among groups assessed using the log-rank test. IB, ibrutinib.

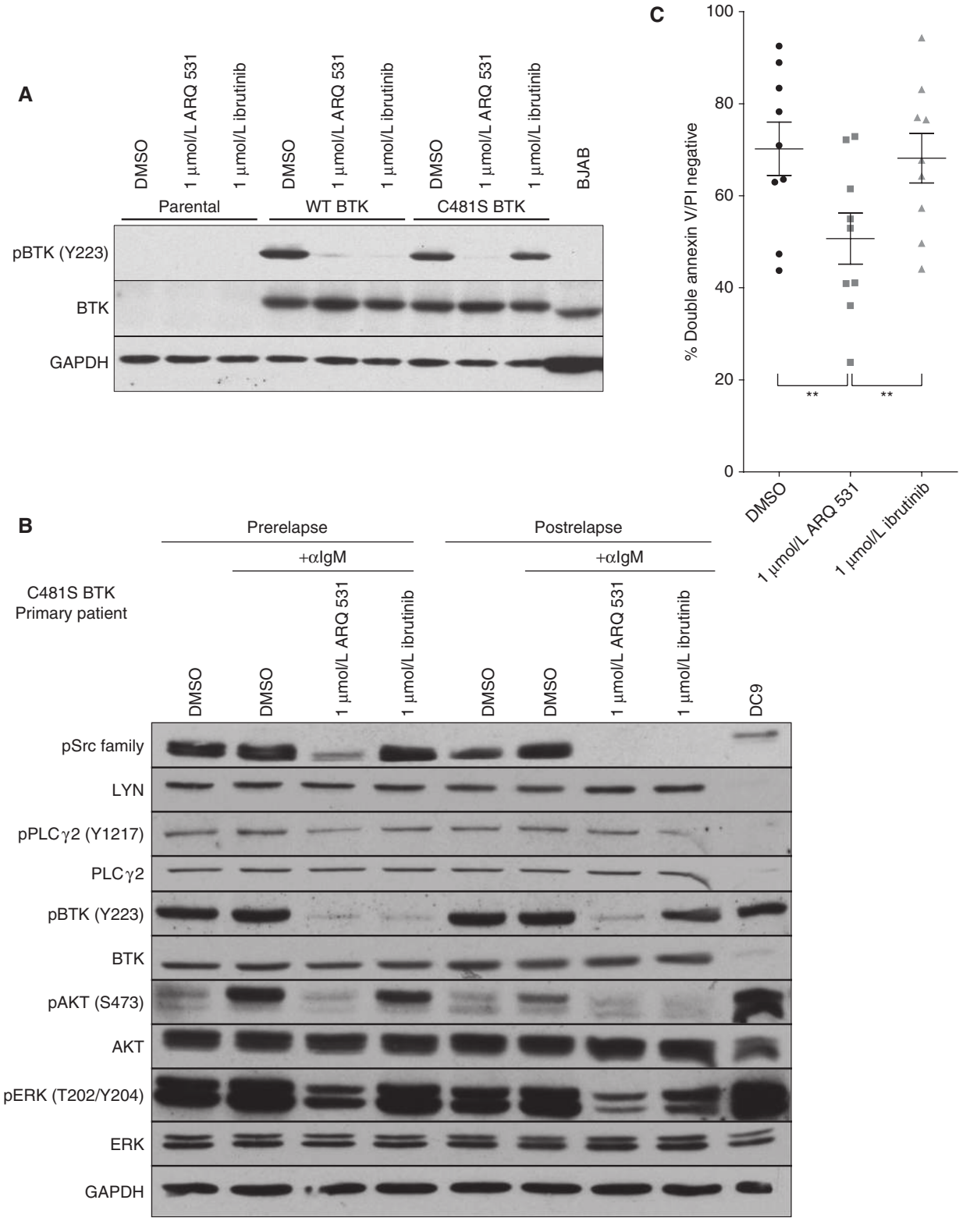

Figure 6. C481S BTK is inhibited by ARQ 531. **A,** A HEK293T cell line stably transfected with wild-type (WT) or C481S BTK was treated with ARQ 531 or ibrutinib for 1 hour followed by SDS-PAGE to determine efficacy against C481S BTK. **B,** CLL cells isolated at baseline and time of progression from an ibrutinib-resistant patient who acquired a C481S BTK mutation were treated with ARQ 531 for 1 hour followed by SDS-PAGE. **C,** Primary CLL cells isolated from ibrutinib-resistant patients who all possessed BTK C481S mutations were treated with ARQ 531 for 72 hours to determine cytotoxicity ($n = 9$). Differences were assessed using linear mixed-effects models (**, $0.01 \geq P \geq 0.001$).

whereas there was no cytotoxicity following ibrutinib treatment ($P = 0.906$; Fig. 6C).

ARQ 531 Effectively Inhibits Downstream Signaling in Ibrutinib-Resistant PLCγ2 Mutants

Previous work has shown that PLCγ2 can be directly activated by LYN and SYK in ibrutinib-refractory models possessing mutant PLCγ2, effectively bypassing the role of BTK in PLCγ2 activation (25). Due to its direct inhibition of LYN and MEK1 and its indirect inhibition of SYK, we hypothesized that ARQ 531 may provide effective inhibition of downstream BCR signaling in patients with mutations in the autoinhibitory domain of PLCγ2. To test this hypothesis, we utilized a *PLCγ2*$^{-/-}$ DT40 cell line transfected with wild-type PLCγ2, R665W PLCγ2, or L845F PLCγ2. We found that ARQ 531 successfully inhibited the downstream activation of ERK in these cell lines, whereas ibrutinib was ineffective (Fig. 7A). To validate this finding, we tested ARQ 531 *in vitro* in CLL cells from a patient with an R665W PLCγ2 mutation acquired following ibrutinib treatment. We found that ARQ 531 preserved BTK, SYK, and ERK inhibition after relapse, whereas ibrutinib was able to inhibit only BTK (Fig. 7B). These results were further confirmed in an ibrutinib-refractory patient possessing multiple PLCγ2 mutations (R665W, S707P, S707F, R742P, and L845fs) in which we found that ARQ 531 preserved BTK, SYK, AKT, and ERK inhibition, whereas ibrutinib was able to inhibit only BTK (Fig. 7C).

DISCUSSION

Due to its unique BTK binding affinity and distinct kinase profile, ARQ 531 is an attractive molecule to study in ibrutinib-resistant CLL, which progresses due to acquired mutations in *BTK* and *PLCγ2* or Richter transformation. Herein, we demonstrate that ARQ 531 maintains inhibitory pressure on the BCR pathway in situations of C481S BTK and autoactivating PLCγ2 mutations. Furthermore, ARQ 531 was found to significantly prolong survival over ibrutinib in a murine model of Richter transformation. The clinical success of ibrutinib has established that BCR signaling is vital to CLL progression and that inhibition of BTK is a successful therapeutic paradigm. Although previous work with the XID mouse model suggests that BTK inhibition alone is sufficient to delay disease progression (2), the extent to which inhibition of additional kinases may affect disease progression is unknown. It is reasonable that combining additional inhibitory pressure on the BCR pathway via kinases both upstream and downstream of BTK might improve efficacy, as is suggested by our *in vivo* experiment using the Eμ-TCL1 mouse model. These data challenge the convention that highly selective inhibition of a single target should serve as the model of drug development for patients with CLL who are resistant to current therapies.

Patients who relapse on ibrutinib progress rapidly and have limited therapeutic options. Although venetoclax has been shown to be effective in this setting (39), not all patients respond, and long-term remissions are uncommon. Given the importance of BCR signaling in CLL progression, it is unsurprising that CLL progression in patients receiving ibrutinib is overwhelmingly mediated by mutation of BTK at its ibrutinib binding site or in the autoinhibitory domain of BTK's immediate downstream signaling partner PLCγ2 (25, 26). Because the BCR pathway remains active in patients who relapse on ibrutinib (40), continuing to inhibit BTK and associated kinases through alternate mechanisms is of great clinical interest and may provide an alternative strategy for long-term disease control. Unlike ibrutinib, ARQ 531 reversibly inhibits BTK and does not require stabilization from C481 to block BTK-mediated signaling. We therefore hypothesized, and found, that ARQ 531 would be effective in models of ibrutinib resistance containing the recurrent C481S BTK mutation. ARQ 531 was also found to inhibit downstream BCR signaling in models expressing activating PLCγ2 mutations. This is likely due to inhibition of SYK and LYN, which have been shown to directly activate PLCγ2 in the setting of activating *PLCγ2* mutations (25). Activity against both C481S BTK and mutated PLCγ2 distinguishes ARQ 531 from other BTK inhibitors currently in preclinical and clinical development.

Another critical area of unmet need in CLL is Richter transformation, where survival is uniformly poor and current therapies are inadequate. Based on our data in the Eμ-MYC/TCL1 mouse, ARQ 531 may be an effective therapy in patients with aggressive lymphomas, including those with Richter transformation. Considering that ibrutinib does not directly inhibit members of the RAS/RAF pathway, it is possible that the superior efficacy of ARQ 531 in the setting of Richter transformation may be due to its inhibition of distal targets including MEK1, which has been shown to be an effective target in diffuse large B-cell lymphomas (41). Inhibiting a broader spectrum of targets may lead to deeper and more durable remissions while delaying the emergence of resistance.

Ibrutinib induces durable responses and extends disease remission in malignancies, including CLL, mantle cell lymphoma, and Waldenström macroglobulinemia, in part through its inhibition of BTK. Because ARQ 531 inhibits BTK with comparable potency, it is expected that ARQ 531 may also be effective in these B-cell malignancies. Furthermore, its inhibition of additional targets and its efficacy in the Eμ-MYC/TCL1 mouse model suggest that ARQ 531 may possess activity in malignancies ineffectively treated by ibrutinib or other BTK inhibitors. Among the most intriguing additional targets of ARQ 531 is MEK1, a constituent of the ERK signaling pathway that is upregulated in ibrutinib-treated CLL cells (42). ERK signaling is of general interest in hematologic malignancies as well as solid tumors due to its ability to influence proliferation and its high frequency of mutation in cancer. RAF1 and MEK1 have been shown to be important targets in the setting of *RAS* mutations (43), which suggests that ARQ 531 may be applicable to RAS-mutated malignancies, including multiple myeloma (44, 45), melanoma (46), and others (47). Moreover, indirect inhibition of SYK by ARQ 531 may allow this molecule to be utilized in the setting of acute myeloid leukemia where SYK inhibition has been shown to impair leukemia progression (48–50). A rationale therefore exists to explore the effect of ARQ 531 in additional malignancies.

Our preclinical studies with ARQ 531 demonstrate that this compound is an effective ATP-competitive kinase

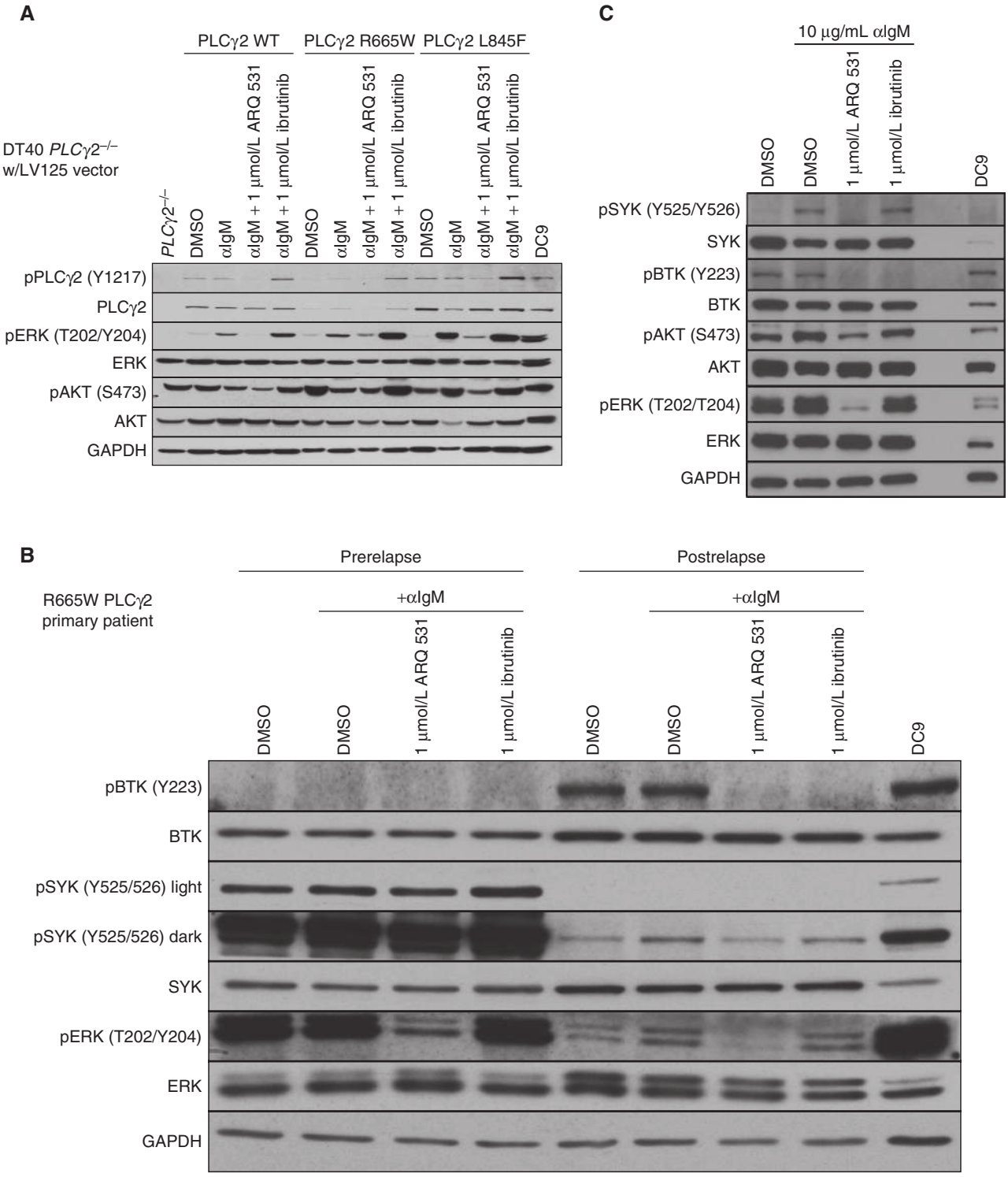

Figure 7. ARQ 531 inhibits BCR signaling in cells with ibrutinib-resistant *PLCγ2* mutations. **A,** A DT40 cell line stably transfected with WT, R665W, or L845F PLCγ2 and treated with ARQ 531 was assessed via SDS-PAGE to determine the effect on activation of the downstream kinases ERK and AKT. **B,** CLL cells isolated from an ibrutinib-resistant patient harboring an R665W PLCγ2 mutation were treated with ARQ 531 followed by SDS-PAGE and assessed for distal BCR signaling. **C,** CLL cells isolated from an ibrutinib-resistant patient harboring multiple *PLCγ2* mutations were treated with ARQ 531 followed by SDS-PAGE and assessed for distal BCR signaling.

inhibitor in the context of ibrutinib-naïve CLL as well as ibrutinib-resistant disease in the form of acquired mutations in *BTK* and/or *PLCγ2* or Richter transformation. Especially in post-ibrutinib patients who tend to have genomically complex disease, a multitargeted agent such as ARQ 531 may be ideal. However, careful attention will need to be paid to toxicity in the phase I setting, as inhibition of multiple kinases could lead to increased toxicity over what is seen with a more selective BTK inhibitor. It will be especially important to ensure that hematopoietic progenitor cells are not inhibited, although this specific toxicity has not been suggested in preclinical studies. The improved survival associated with ARQ 531 treatment in multiple murine models suggests that less discriminating kinase inhibitors may deserve additional consideration in the development of therapies for this purpose and potentially other malignancies. Our findings justify continued preclinical work on ARQ 531 and investigation in human clinical trials for CLL and Richter transformation.

METHODS

Subject Population and Lymphocyte Isolation

Blood was obtained from patients with CLL at our institution, who consented to an Institutional Review Board (IRB)–approved tissue procurement protocol or who were enrolled in IRB-approved clinical trials of ibrutinib in CLL that allowed tissue procurement for research purposes. All patients provided written informed consent in accordance with the Declaration of Helsinki. Peripheral blood mononuclear cells (PBMC) were isolated from whole blood through Ficoll density gradient centrifugation. B cells from patients with CLL were negatively selected using Rosette-Sep isolation from whole blood or Easy-Sep negative selection from PBMCs (STEMCELL Technologies).

BTK Biochemical and Kinase Selectivity Assay

Biochemical inhibition of BTK was measured using full-length BTK constructs of wild-type and C481S-mutant proteins (Reaction Biology). ARQ 531 was tested in a 10-point concentration mode with 3-fold serial dilutions starting at 1 μmol/L in the presence of 10 μmol/L ATP, and the IC_{50} was determined. Kinase selectivity against 236 kinases at 200 nmol/L concentration of ARQ 531 was performed at Millipore Sigma. The IC_{50} values for the off-target kinases were determined at a physiologic 1 mmol/L ATP concentration (Carna Biosciences).

Crystal Structure Determination

Kinase domain of BTK (387-659) was expressed as a 6xHis-tagged protein in Sf9 insect cells, and the protein was purified on a Ni-NTA column ion exchange and size exclusion chromatography. Crystals were obtained by the hanging drop method. Initially, apo-BTK kinase domain crystals were obtained from drops containing 0.2M imidazole pH 7.0, 16% (w/v) PEG 4000, and 12.5% ethylene glycol at 4°C. Subsequently, the BTK–ARQ 531 complex was generated by microseeding of the apo-BTK crystals. Data to 1.1 Å were collected at 100K at station I03 (λ = 0.9763 Å), Diamond Light Source equipped with a Pilatus3 6M detector.

Cell Culture and Drug Treatment

RPMI-1640 medium supplemented with 100 U/mL penicillin, 100 μg/mL streptomycin, and 10% fetal bovine serum (FBS) was used for cell cultures. To specifically inhibit the irreversible targets of ibrutinib, cells were treated with ibrutinib for 1 hour followed by washout, in which cells were pelleted and resuspended in fresh media. Cells treated with DMSO or ARQ 531 were pelleted and then resuspended in 10% FBS RPMI-1640 media containing DMSO or ARQ 531. Cells used in experiments that occurred over multiple days received fresh media and drug every 24 hours. ARQ 531 ((2-chloro-4-phenoxyphenyl)(4-(((3R,6S)-6-(hydroxymethyl)tetrahydro-2H-pyran-3-yl)amino)-7H-pyrrolo[2,3-d]pyrimidin-5-yl)methanone) was supplied by ArQule Inc.

Immunoblotting

Freshly isolated patient CLL cells treated with ARQ 531 or ibrutinib were stimulated by spinning onto a 6-well plate coated with anti-IgM antibody (The Jackson Laboratory) at a concentration of 10 μg/mL. Following 15 minutes of stimulation, cell lysates were collected and analyzed by SDS-PAGE. Blots were probed with primary antibodies and horseradish peroxidase–conjugated secondary antibodies (Santa Cruz Biotechnologies), and then visualized with SuperSignal chemiluminescent substrate (Thermo Fisher Scientific) on X-ray film. The following antibodies obtained from Cell Signaling Technologies were utilized for immunoblot experiments: anti-phospho-BTK (Y223, cat. #5082), anti-BTK (cat. #8547), anti-phospho-PLCγ2 (Y1217, cat. #3871), anti-PLCγ2 (cat. #3872), anti-phospho-AKT (S473, cat. #9271), anti-AKT (cat. #4685), anti-phospho-ERK (T202/Y204, cat. #9101), anti-ERK (cat. #4695), anti-phospho-MEK1/2 (S217/221, cat. #9121), anti-MEK1/2 (cat. #8727), anti-phospho-SYK (Y525/526, cat. #2710), anti-SYK (cat. #2712), anti-phospho-Src family (Y416, cat. #2101), anti-LYN (cat. #2796), anti-phospho-IKBa (S32, cat. #2859), anti-IKBa (cat. #4812), anti-GAPDH (cat. #5179), anti-Lamin (cat. #13435), and anti-p65 (8242). Anti-phospho-BTK (Y551, cat. #MAB7659) was ordered from R&D Systems. BJAB and DC9 cell line lysates were used as positive controls.

Viability

Viability of patient CLL cells was determined by annexin V and propidium iodide staining (eBioscience) followed by flow cytometry analysis. Viability was defined as the percentage of cells staining dually negative for both annexin V and propidium iodide. All viability measurements were acquired with a Beckman Coulter FC500 flow cytometer, and Kaluza software (Beckman Coulter) was used for data analysis.

Migration

Following treatment with ARQ 531 or ibrutinib, CLL cells were placed into an 8.0-μm transwell insert (Sigma-Aldrich) resting in media containing 200 ng/mL CXCL12 (R&D Systems) or 1 μg/mL CXCL13 (R&D Systems). After incubating for 4 hours, the inserts were removed, and the number of cells migrating through the transwell insert toward CXCL12 or CXCL13 was counted by flow cytometry and normalized to input controls. Data analysis was conducted using Kaluza software.

CpG-Induced Activation

Following treatment with DMSO, ARQ 531, or ibrutinib, CLL cells were stimulated with 3.2 μg/mL oligodeoxynucleotide CpG (Eurofins MWG Operon). Subsequent expression of CD40 and CD86 was determined by mean fluorescence intensity (MFI) after 48 hours with a CD40-PE– or CD86-PE–conjugated antibody (BD Biosciences). Staining intensity of CD40-PE and CD86-PE was measured using a Beckman Coulter FC3000 flow cytometer, and data analysis was conducted using Kaluza software.

RT-PCR

CLL cells were treated with DMSO, ARQ 531, or ibrutinib for 72 hours prior to TRIzol lysis and RNA purification via an RNeasy

isolation kit (Qiagen). Lysates were analyzed for mRNA expression via RT-PCR using the following Applied Biosystems primers and probes: *MCL1* (cat. # Hs01050896_m1), *MYC* (cat. # Hs00153408_m1), *CD40* (cat. # Hs01002915_g1), and *TBP* (cat. # Hs00427620_m1). RNA expression was measured using a Viia7 Real-Time PCR system and normalized against TBP expression.

Eμ-TCL1 Mouse Model

C57BL/6 mice were engrafted via tail-vein injection with 1E7 live $CD5^+/CD19^+$ B cells isolated from the spleen of a single Eμ-TCL1 mouse. Once a peripheral population of $CD5^+/CD19^+$ cells was established at greater than 10%, the mice were randomly assigned to experimental cohorts. Mice were treated with vehicle consisting of 10% Cremophor EL and 10% ethanol in saline, 75 mg/kg ARQ 531, 50 mg/kg ARQ 531, or 25 mg/kg ibrutinib via daily oral gavage and tracked for overall survival. Two concentrations of ARQ 531 were chosen to assess efficacy and potential drug-related toxicity, and 25 mg/kg of ibrutinib has been established as an effective concentration for use in this model. Weekly bleeding was performed in order to assess $CD5^+/CD19^+$ cell populations and to prepare slides for microscopic examination. Cessation of drug treatment occurred at 74 days.

Eμ-MYC/TCL1 Mouse Model

C57BL/6 mice were engrafted via tail-vein injection with 5E6 live $CD5^+/CD19^+$ B cells isolated from the spleen of a single Eμ-Myc/TCL1 donor mouse. Ten days following engraftment, mice were randomly assigned to experimental cohorts. Mice were treated with vehicle, 75 mg/kg ARQ 531, or 25 mg/kg ibrutinib via daily oral gavage and tracked for overall survival. Weekly bleeding was performed in order to assess $CD5^+/CD19^+$ cell populations and to prepare slides for microscopic examination.

Statistical Analysis

Differences in phosphorylation (Fig. 2B), cytotoxicity (Figs. 3A and B, and 6C), transcript expression (ΔCt values; Fig. 3C), CD40/CD86 MFI (log-transformed values; Fig. 3D and E), and migration toward CXCL12/CXCL13 (log-transformed values; Fig. 3F and G) between groups were estimated using mixed models to account for correlations among observations from the same patient. Survival curves were estimated using the Kaplan–Meier method, and curve differences between groups were assessed using the log-rank test (Figs. 4A and 5A). ANOVA was used to compare spleen weight (Fig. 4C) among groups. Mixed-effects models were also used to compare group differences in the percentage of $CD19^+$ cells over time (Fig. 5B). Data represent mean ± SEM. For experiments with multiple endpoints, *P* values were adjusted for multiple comparisons using Holm's procedure. All analyses were performed using SAS/STAT software, version 9.4 of the SAS system for Windows (SAS Institute, Inc.).

Study Approval

All studies conducted with the use of human samples were reviewed and approved by The Ohio State University IRB. Animal experiments were conducted in accordance with the guidelines established by The Ohio State University and approved by the Institutional Animal Care and Use Committee.

Disclosure of Potential Conflicts of Interest

K.A. Rogers is a consultant/advisory board member for Acerta Pharma. F.T. Awan reports receiving a commercial research grant from Pharmacyclics and is a consultant/advisory board member for Pharmacyclics, Gilead, and AbbVie. K. Maddocks is a consultant/advisory board member for Pharmacyclics and AstraZeneca. G. Abbadessa has ownership interest (including stock, patents, etc.) in ArQule. B. Schwartz has ownership interest (including stock, patents, etc.) in ArQule. J.A. Woyach reports receiving commercial research support from Acerta, Karyopharm, Morphosys, and Janssen. No potential conflicts of interest were disclosed by the other authors.

Authors' Contributions

Conception and design: S.D. Reiff, S. Eathiraj, G. Abbadessa, B. Schwartz, A.J. Johnson, J.C. Byrd, J.A. Woyach

Development of methodology: S.D. Reiff, J.T. Greene, S. Eathiraj, G. Abbadessa, J.C. Byrd, J.A. Woyach

Acquisition of data (provided animals, acquired and managed patients, provided facilities, etc.): S.D. Reiff, R. Mantel, L.L. Smith, E.M. Muhowski, C.A. Fabian, V.M. Goettl, M. Tran, B.K. Harrington, K.A. Rogers, K. Maddocks, L. Andritsos, S. Eathiraj, J.C. Byrd, J.A. Woyach

Analysis and interpretation of data (e.g., statistical analysis, biostatistics, computational analysis): S.D. Reiff, J.T. Greene, B.K. Harrington, K.A. Rogers, A.M. Lehman, R. Lapalombella, S. Eathiraj, G. Abbadessa, B. Schwartz, J.C. Byrd

Writing, review, and/or revision of the manuscript: S.D. Reiff, C.A. Fabian, V.M. Goettl, B.K. Harrington, K.A. Rogers, F.T. Awan, A.M. Lehman, D. Sampath, R. Lapalombella, S. Eathiraj, G. Abbadessa, B. Schwartz, A.J. Johnson, J.C. Byrd, J.A. Woyach

Administrative, technical, or material support (i.e., reporting or organizing data, constructing databases): R. Mantel, E.M. Muhowski, F.T. Awan, S. Eathiraj, B. Schwartz, J.C. Byrd, J.A. Woyach

Study supervision: S. Eathiraj, J.C. Byrd, J.A. Woyach

Other (dosed, accessed disease status, and collected blood during study, determined removal endpoint, euthanized, and collected tissue): V.M. Goettl

Acknowledgments

ARQ 531 was provided by ArQule Inc. This research was supported by grants from the NIH (J.A Woyach, K23 CA178183 and R01 CA197870; J.C. Byrd, R35 CA197734 and P30 CA016058).

The costs of publication of this article were defrayed in part by the payment of page charges. This article must therefore be hereby marked *advertisement* in accordance with 18 U.S.C. Section 1734 solely to indicate this fact.

Received February 2, 2018; revised May 14, 2018; accepted August 2, 2018; published first August 9, 2018.

REFERENCES

1. Packham G, Stevenson F. The role of the B-cell receptor in the pathogenesis of chronic lymphocytic leukaemia. Semin Cancer Biol 2010;20:391–9.
2. Woyach JA, Bojnik E, Ruppert AS, Stefanovski MR, Goettl VM, Smucker KA, et al. Bruton's tyrosine kinase (BTK) function is important to the development and expansion of chronic lymphocytic leukemia (CLL). Blood 2014;123:1207–13.
3. Advani RH, Buggy JJ, Sharman JP, Smith SM, Boyd TE, Grant B, et al. Bruton tyrosine kinase inhibitor ibrutinib (PCI-32765) has significant activity in patients with relapsed/refractory B-cell malignancies. J Clin Oncol 2013;31:88–94.
4. Byrd JC, Brown JR, O'Brien S, Barrientos JC, Kay NE, Reddy NM, et al. Ibrutinib versus ofatumumab in previously treated chronic lymphoid leukemia. N Engl J Med 2014;371:213–23.
5. Burger JA, Tedeschi A, Barr PM, Robak T, Owen C, Ghia P, et al. Ibrutinib as initial therapy for patients with chronic lymphocytic leukemia. N Engl J Med 2015;373:2425–37.

6. Byrd JC, Harrington B, O'Brien S, Jones JA, Schuh A, Devereux S, et al. Acalabrutinib (ACP-196) in relapsed chronic lymphocytic leukemia. N Engl J Med 2016;374:323–32.
7. Walter HS, Rule SA, Dyer MJ, Karlin L, Jones C, Cazin B, et al. A phase 1 clinical trial of the selective BTK inhibitor ONO/GS-4059 in relapsed and refractory mature B-cell malignancies. Blood 2016;127:411–9.
8. Tam C, Grigg AP, Opat S, Ku M, Gilbertson M, Anderson MA, et al. The BTK inhibitor, Bgb-3111, is safe, tolerable, and highly active in patients with relapsed/refractory B-cell malignancies: initial report of a phase 1 first-in-human trial. Blood (ASH Annual Meeting Abstracts) 2015;126:832.
9. Woyach JA, Johnson AJ, Byrd JC. The B-cell receptor signaling pathway as a therapeutic target in CLL. Blood 2012;120:1175–84.
10. Lougaris V, Baronio M, Vitali M, Tampella G, Cattalini M, Tassone L, et al. Bruton tyrosine kinase mediates TLR9-dependent human dendritic cell activation. J Allergy Clin Immunol 2014;133:1644–50 e1644.
11. Lee KG, Xu S, Wong ET, Tergaonkar V, Lam KP. Bruton's tyrosine kinase separately regulates NFkappaB p65RelA activation and cytokine interleukin (IL)-10/IL-12 production in TLR9-stimulated B Cells. J Biol Chem 2008;283:11189–98.
12. de Gorter DJ, Beuling EA, Kersseboom R, Middendorp S, van Gils JM, Hendriks RW, et al. Bruton's tyrosine kinase and phospholipase Cgamma2 mediate chemokine-controlled B cell migration and homing. Immunity 2007;26:93–104.
13. Chen SS, Chang BY, Chang S, Tong T, Ham S, Sherry B, et al. BTK inhibition results in impaired CXCR4 chemokine receptor surface expression, signaling and function in chronic lymphocytic leukemia. Leukemia 2016;30:833–43.
14. Herman SE, Gordon AL, Hertlein E, Ramanunni A, Zhang X, Jaglowski S, et al. Bruton tyrosine kinase represents a promising therapeutic target for treatment of chronic lymphocytic leukemia and is effectively targeted by PCI-32765. Blood 2011;117:6287–96.
15. Herman SE, Sun X, McAuley EM, Hsieh MM, Pittaluga S, Raffeld M, et al. Modeling tumor-host interactions of chronic lymphocytic leukemia in xenografted mice to study tumor biology and evaluate targeted therapy. Leukemia 2013;27:1769–73.
16. O'Brien S, Furman R, Coutre S, Flinn IW, Burger J, Blum K, et al. Five-year experience with single agent ibrutinib in patients with previously untreated and relapsed/refractory chronic lymphocytic leukemia/small lymphocytic lymphoma. Blood (ASH Annual Meeting Abstracts). 2016:Abstract 233.
17. Woyach JA, Ruppert AS, Guinn D, Lehman A, Blachly JS, Lozanski A, et al. BTKC481S-mediated resistance to ibrutinib in chronic lymphocytic leukemia. J Clin Oncol 2017;35:1437–43.
18. Maddocks KJ, Ruppert AS, Lozanski G, Heerema NA, Zhao W, Abruzzo L, et al. Etiology of ibrutinib therapy discontinuation and outcomes in patients with chronic lymphocytic leukemia. JAMA oncology 2015;1:80–7.
19. Ahn IE, Tian X, Soto S, Valdez J, Lotter J, Farooqui M, et al. Prognostic models predictive of disease progression in CLL patients treated with ibrutinib blood (ASH Annual Meeting Abstracts). 2016:Abstract 187.
20. Parikh SA, Chaffee KR, Call TG, Ding W, Leis JF, Chanan-Khan A, et al. Ibrutinib therapy for chronic lymphocytic leukemia (CLL): an analysis of a large cohort of patients treated in routine clinical practice. Blood (ASH Annual Meeting Abstracts) 2015;126:Abstract 2935.
21. Sandoval-Sus JD, Chavez JC, Dalia S, Bello CM, Shah BD, Ho VQ, et al. Outcomes of patients with relapsed/refractory chronic lymphocytic leukemia after ibrutinib discontinuation outside clinical trials: a single institution experience. Blood (ASH Annual Meeting Abstracts) 2015;126:Abstract 2945.
22. Jain P, Keating M, Wierda W, Estrov Z, Ferrajoli A, Jain N, et al. Outcomes of patients with chronic lymphocytic leukemia after discontinuing ibrutinib. Blood 2015;125:2062–7.
23. Woyach JA, Furman RR, Liu TM, Ozer HG, Zapatka M, Ruppert AS, et al. Resistance mechanisms for the Bruton's tyrosine kinase inhibitor ibrutinib. N Engl J Med 2014;370:2286–94.
24. Furman RR, Cheng S, Lu P, Setty M, Perez AR, Guo A, et al. Ibrutinib resistance in chronic lymphocytic leukemia. N Engl J Med 2014;370:2352–4.
25. Liu TM, Woyach JA, Zhong Y, Lozanski A, Lozanski G, Dong S, et al. Hypermorphic mutation of phospholipase C, gamma2 acquired in ibrutinib-resistant CLL confers BTK independency upon B-cell receptor activation. Blood 2015;126:61–8.
26. Jones D, Woyach JA, Zhao W, Caruthers S, Tu H, Coleman J, et al. PLCG2 C2 domain mutations co-occur with BTK and PLCG2 resistance mutations in chronic lymphocytic leukemia undergoing ibrutinib treatment. Leukemia 2017;31:1645–7.
27. Rogers KA, El-Gamal D, Bonnie HK, Zachary HA, Virginia GM, Rose M, et al. The Eμ-Myc/TCL1 transgenic mouse as a new aggressive B-cell malignancy model suitable for preclinical therapeutics testing. Blood 2015;126:2752–2.
28. Bichi R, Shinton SA, Martin ES, Koval A, Calin GA, Cesari R, et al. Human chronic lymphocytic leukemia modeled in mouse by targeted TCL1 expression. PNAS 2002;99:6955–60.
29. Bender AT, Gardberg A, Pereira A, Johnson T, Wu Y, Grenningloh R, et al. Ability of Bruton's tyrosine kinase inhibitors to sequester Y551 and prevent phosphorylation determines potency for Inhibition of Fc receptor but not B-cell receptor signaling. Mol Pharmacol 2017;91:208–19.
30 Eid S, Turk S, Volkamer A, Rippmann F, Fulle S. KinMap: a web-based tool for interactive navigation through human kinome data. BMC Bioinformatics 2017;18:16.
31. Browning RL, Mo X, Muthusamy N, Byrd JC. CpG oligodeoxynucleotide CpG-685 upregulates functional interleukin-21 receptor on chronic lymphocytic leukemia B cells through an NF-kappaB mediated pathway. Oncotarget 2015;6:15931–9.
32. Ponader S, Chen SS, Buggy JJ, Balakrishnan K, Gandhi V, Wierda WG, et al. The Bruton tyrosine kinase inhibitor PCI-32765 thwarts chronic lymphocytic leukemia cell survival and tissue homing in vitro and in vivo. Blood 2012;119:1182–9.
33. de Rooij MF, Kuil A, Geest CR, Eldering E, Chang BY, Buggy JJ, et al. The clinically active BTK inhibitor PCI-32765 targets B-cell receptor- and chemokine-controlled adhesion and migration in chronic lymphocytic leukemia. Blood 2012;119:2590–4.
34. Woyach JA, Guinn D, Ruppert AS, Blachly JS, Lozanski A, Heerema NA, et al. the development and expansion of resistant subclones precedes relapse during ibrutinib therapy in patients with CLL. Blood 2016;128:55.
35. Herman SEM, Montraveta A, Niemann CU, Mora-Jensen H, Gulrajani M, Krantz F, et al. The Bruton tyrosine kinase (BTK) inhibitor acalabrutinib demonstrates potent on-target effects and efficacy in two mouse models of chronic lymphocytic leukemia. Clin Cancer Res 2017;23:2831–41.
36. Eathiraj S, Savage R, Yu Y, Schwartz B, Woyach J, Johnson A, et al. Targeting ibrutinib-resistant BTK-C481S mutation with ARQ 531, a reversible non-covalent inhibitor of BTK. Soc Hematol Oncol Ann Meeting 2016;16(S47–S48).
37. Hall T, Eathiraj S, Stephens DM, Woyach J, Flinn IW, Savage R, et al. ARQ 531, a novel and reversible inhibitor of Bruton's tyrosine kinase, displays favorable oral bioavailability and exposure in patients with B-cell malignancies. American Association of Cancer Research Annual Meeting 2018;Abstract LB-018.
38. Marostica E, Sukbuntherng J, Loury D, de Jong J, de Trixhe XW, Vermeulen A, et al. Population pharmacokinetic model of ibrutinib, a Bruton tyrosine kinase inhibitor, in patients with B cell malignancies. Cancer Chemother Pharmacol 2015;75:111–21.
39. Jones JA, Mato AR, Wierda WG, Davids MS, Choi M, Cheson BD, et al. Venetoclax for chronic lymphocytic leukaemia progressing after ibrutinib: an interim analysis of a multicentre, open-label, phase 2 trial. Lancet 2018;19:65–75.
40. Cheng S, Guo A, Lu P, Ma J, Coleman M, Wang YL. Functional characterization of BTK(C481S) mutation that confers ibrutinib resistance: exploration of alternative kinase inhibitors. Leukemia 2015;29:895–900.
41. Bhalla S, Evens AM, Dai B, Prachand S, Gordon LI, Gartenhaus RB. The novel anti-MEK small molecule AZD6244 induces BIM-

dependent and AKT-independent apoptosis in diffuse large B-cell lymphoma. Blood 2011;118:1052–61.
42. Woyach JA, Smucker K, Smith LL, Lozanski A, Zhong Y, Ruppert AS, et al. Prolonged lymphocytosis during ibrutinib therapy is associated with distinct molecular characteristics and does not indicate a suboptimal response to therapy. Blood 2014;123:1810–7.
43. Lamba S, Russo M, Sun C, Lazzari L, Cancelliere C, Grernrum W, et al. RAF suppression synergizes with MEK inhibition in KRAS mutant cancer cells. Cell reports 2014;8:1475–83.
44. Bezieau S, Devilder MC, Avet-Loiseau H, Mellerin MP, Puthier D, Pennarun E, et al. High incidence of N and K-Ras activating mutations in multiple myeloma and primary plasma cell leukemia at diagnosis. Hum Mutat 2001;18:212–24.
45. de la Puente P, Muz B, Jin A, Azab F, Luderer M, Salama NN, et al. MEK inhibitor, TAK-733 reduces proliferation, affects cell cycle and apoptosis, and synergizes with other targeted therapies in multiple myeloma. Blood Cancer J 2016;6:e399.
46. Vu HL, Aplin AE. Targeting mutant NRAS signaling pathways in melanoma. Pharmacol Res 2016;107:111–6.
47. Prior IA, Lewis PD, Mattos C. A comprehensive survey of Ras mutations in cancer. Cancer Res 2012;72:2457–67.
48. Boros K, Puissant A, Back M, Alexe G, Bassil CF, Sinha P, et al. Increased SYK activity is associated with unfavorable outcome among patients with acute myeloid leukemia. Oncotarget 2015;6:25575–87.
49. Carnevale J, Ross L, Puissant A, Banerji V, Stone RM, DeAngelo DJ, et al. SYK regulates mTOR signaling in AML. Leukemia 2013;27:2118–28.
50. Walker AR, Bhatnagar B, Marcondes AM, DiPaolo J, Vasu S, Mims AS, et al. Interim results of a phase 1b/2 study of entospletinib (GS-9973) monotherapy and in combination with chemotherapy in patients with acute myeloid leukemia. Blood (American Society of Hematology Annual Meeting Abstracts) 2016;128:2831.